

DEUTSCHES ELEKTRONEN-SYNCHROTRON **DESY**

DESY 76/05
January 1976



Particle Identification with a Liquid Argon Ionization Chamber

by

Gerhard Knies

Deutsches Elektronen-Synchrotron DESY, Hamburg

Ulrich Glawe

II. Institut für Experimentalphysik der Universität Hamburg

2 HAMBURG 52 NOTKESTIEG 1

To be sure that your preprints are promptly included in the
HIGH ENERGY PHYSICS INDEX,
send them to the following address (if possible by air mail):

DESY
Bibliothek
2 Hamburg 52
Notkestieg 1
Germany

PARTICLE IDENTIFICATION WITH A LIQUID ARGON IONIZATION CHAMBER

by

Gerhard Knies

Deutsches Elektronen-Synchrotron DESY, Hamburg

Ulrich Glawe

II. Institut für Experimentalphysik der Universität Hamburg

Abstract

The electric charge as produced by ionizing pions and protons in liquid argon has been measured for particle momenta up to 1.3 GeV/c. Using the correlated signals from two consecutive chambers we have determined the probability for a pion to simulate a proton. Up to 1.3 GeV/c the pion peak and the proton peak were separated in the ionization spectrum. Applications of this method for particle identification and for charge measurement are discussed.

Introduction

Ionization measurements in liquid argon¹⁻³⁾ are going to come into a widespread use in calorimeters to measure the energy of hadronic and electromagnetic showers. This development is mainly due to the experimental conditions and requirements of storage ring experiments.⁴⁾ In this article we want to report on the possibility of using liquid argon ionization chambers (LARICs) for particle identification.

The development of this novel method was motivated mainly by its advantages for storage ring detectors. LARICs can be used for particle identification and charge measurement under the following circumstances:

- 1) separation of integrally charged nonrelativistic particles (π , K, p) in combination with a momentum measurement
- 2) direct charge measurement of relativistic particles
- 3) determination of mass and charge for non-relativistic particles in combination with a time of flight and momentum measurement.

In addition to these fundamental properties we want to point out that it looks simple to extend LARICs over a solid angle of almost 4π , to incorporate them into magnetic detectors, and to realize an area segmentation into elements that adjusts to very specific experimental conditions.

For these reasons it seemed worthwhile to demonstrate that this novel detector is practical. In Section II we present some of the design considerations for the LARICs and in Section III we describe the construction of the chamber and the electronics. In Section IV and V the test run and the results are described. In Section VI we discuss some applications.

II. Design Considerations for a LARIC

There are two dominating effects that limit the resolution in dE/dx measurements by a LARIC:

- 1) The δ -rays (Landau fluctuations)
- 2) Electronic noise of the small signal amplifier.

Both of these effects can be brought down to a suitable level by a proper design of the LARIC.

The Landau fluctuation adds to the right hand tail of the ionization distribution (see Fig.5b). This effect increases the fraction of pions producing ionization like a proton of the same momentum. However when using several consecutive gaps (see Fig.1) and selecting the smallest signal (see Fig.2) this effect is greatly reduced. In Table 1 we show results from Monte Carlo calculations of the probability for a 1 GeV/c pion to produce an ionization signal falling into an interval around the proton peak which contains 68% of the protons. According to these calculations the pion rejection is considerably improved when going from 1 to 2 or 4 consecutive gaps. The calculations are well corroborated by the experimental findings for the 1-gap and the 2-gap setups.

To have the electronic noise smaller than 5% of the signals, first of all one chooses low noise amplifiers. Furthermore it is possible to increase the signals by enlarging the depth of the argon gap that the tracks are going to cross and to keep the capacity of the LARIC segment small.

We chose a gap of 10 mm depth together with a 50 by 50 mm² cross section of the sensitive segment (see Fig.1).

The depth of a gap not only affects the size of the signals, but also their build up time. The drift times for a 10 mm deep gap in pure liquid argon for various field strengths are shown in Fig.3. We also show the respective drift times for a mixture of 97% argon and 3% methane.⁵⁾ At field strengths larger than 5 KV/cm the drift time in the mixture comes down to 1/3 of the corresponding figure in pure argon.

In the test run we used pure argon and in general a high voltage of 4.2 KV/cm giving a drift time of 3,5 μ s.

III. The Chamber and the Electronics

The chamber is shown in Fig.1. The electrodes were 1.5 mm thick fibre glass strengthened epoxid plates coated by 35 μ m of copper. The electrodes were held together by nylon bolts and nylon screws at a spacing of 9.9 ± 0.1 mm.

The chamber was enclosed in a leak tight container formed by two stainless steel flanges. The clean argon supply pipe was welded, and the feed throughs for the high voltage and the signal leads were soldered into one of the side caps.

The signals were amplified and analyzed according to the scheme in Fig.2. With calibration pulses the gains for both channels were adjusted to be equal. The total gain was 10^4 . We also used pulse shaping with an integration time of $2 \mu\text{s}$ and a differentiation time of $5 \mu\text{s}$, at drift times of $3.5 \mu\text{s}$.

The track signals from both channels have been analyzed by a pulse height analyzer, either singly or after submission to the smallest signal selecting circuit.

IV. The Test Run

1) The Beam

We have tested the performance of the LARIC double gap detector in the test beam t1 at CERN. The beam can be operated at momenta from $0.4 \text{ GeV}/c$ up to $2.4 \text{ GeV}/c$ for positive or negative particles. The negative beam contains pions only whereas the positive beam consists of pions and protons. There were no other installations for identifying pions and protons in this beam.

2) Operating the Chamber

The LARIC device was sitting in an open bath of (dirty) liquid argon and was connected to a bottle of gaseous clean argon⁶⁾ (see Fig.4). When the chamber was cold, a valve was opened to let in the gaseous argon which then liquified inside the chamber. When the chamber was filled up with the liquid this valve was closed. Control of the liquid inside the LARIC was done by measuring the pressure and manually refilling the cooling bath.

3) Data Taking

Signals were visible from about $500 \text{ V}/\text{cm}$ up. The chamber was operated mainly at 4.2 KV , and some additional measurements were taken at 3 KV and 2 KV to check on the effect of impurities.

The intensity of the beam was such that there was a pile-up problem, i.e. sometimes there was more than one particle crossing within $\sim 10 \mu\text{s}$. In these cases a second pulse is sitting on the decaying preceding one and so pretending

a larger pulse height. This effect increases the apparent pulse height up to 2 times the single track signals. Since the pile-up situation will occur correlated in the two consecutive gaps this effect will not be reduced by the smaller signal selecting circuit.

The π^- pulse height spectrum in Fig.5 shows that the pile-up effect was present but small. This effect of course tends to degrade the proton-pion separation. Under cleaner conditions one therefore might achieve somewhat better values on proton pion separation than the figures we are coming up with from our present measurements.

V. Results

The main results are presented in Fig.6 which shows the pulse height spectra for the positiv beam after the smaller signal selecting circuit, at 6 beam momenta between 800 and 1300 MeV/c.

To demonstrate the effect of the smaller signal selection, we compare in Fig.7 double and single gap pulse height spectra from the same beam setting (1000 MeV/c). In the double gap chamber, the pion background at the proton peak position is down to 1/3 of the corresponding figure for the single gap chamber.

In the double gap chamber two clearly distinct ionization peaks from pions and protons, respectively, are visible when using the smaller signal selecting circuit (Fig.6) for beam momenta less than 1000 MeV/c. Up to 1300 MeV/c it is possible to identify two separate peaks. The variation of the proton ionization peak position with momentum is shown in Fig.8. It compares well with the theoretical expectation. Also shown is the asymmetric half width at half height.

What is the π -p separation in quantitative terms? Using the π^- -pulse height spectrum of Fig.5 as the shape of the π^+ contribution in Fig.6 we have determined the fraction of pions giving a signal of such a size that they fall into that part of the pulse height spectrum where 68% of the proton signals are located. This probability for a pion to look like a proton is shown in Fig.9. At 1000 MeV/c, this probability is 4%.

Finally we would like to mention some further observations:

- 1) The particle separation was limited by the Landau fluctuation rather than by the electronic noise.

- 2) Over the two days period of operation, the whole system worked without any distortion.
- 3) Over the same period the pion peak did not move within $\pm 1\%$, promising a stable mode of operation and an easy calibration for this kind of detector.
- 4) The pion peak was stable within $\pm 1\%$ from 800 MeV/c up to 2 GeV/c. No indication for a relativistic rise was observed.

VI. Applications

1) Particle Identification

This method can be used for low momentum π -K-p separation. The figures for π -K separation can be inferred from the measured π -p figures by the scaling law for ionization. To illustrate what can be accomplished with this method we determine the momenta up to which a π -K separation with a pion background of 1:5, and 1:1, respectively, can be achieved in the 68% kaon interval, assuming a π :K ratio of 5:1 (at around 600 MeV/c.) For the (π, K) -p separation problem we assume a relative (π, K) abundance of 10:1 (at around 1 GeV/c). Under these conditions we find the following results on π -K-p separation:

	for signal: background	
	5:1	1:1
$\pi - K - p$	<500	<700 MeV/c
$(\pi, K) - p$	<820	<1120 MeV/c

These figures correspond to what can be achieved by a time of flight measurement over a drift space of approximately 120 cm.

2) Search for New Particles

This method can be utilized in a search for particles with fractional charge or other unconventional heavy long living particles.

In general quarks can be identified

- 1) by showing an apparant momentum $p' > P_B$, the beam momentum.
A particle with the charge e' shows an apparant momentum of
 $p' = \frac{e'}{e} \cdot p$, with p being the real momentum;
- 2) by showing a ratio $I/I_0 < 1$ with I_0 the minimum ionization of a particle with charge e .

Both of these signatures, however, do not work close above production thresholds, where the momentum p is low and ionization I is more than minimal. Depending on the mass of the quark, only that range of energy might be available in an experiment. More precisely for pair production of quarks at e^+e^- storage rings with a quark mass M_Q and charge $2/3$, these two identification methods work if

$$P_B > 1.33 M_Q \quad \text{to get } p' > P_B$$

$$P_B > 1.22 M_Q \quad \text{to get } I/I_0 < 1$$

For $P_B < 1.22 M_Q$ a quark can be identified if I/I_0 and the time of flight (or the speed β) are measured. At $P_B = 1.22 M_Q$ we have $\beta = 0.57$. What drift space, or a detector of what size is necessary for TOF measurement to separate $\beta = 0.57$ from $\beta = 1$ particles? In a quark search one would like to have a 4 (5) s.d. separation. With a time resolution of $\sigma(\tau) = 0.3$ nsec this leads to a drift space of

$$d = \sqrt{2} \cdot 4(5) \cdot \sigma \cdot \frac{\beta_1 \beta_2}{\Delta\beta} \cdot c = 68(85) \text{ cm.}$$

Therefore a detector with momentum and dE/dx measurement and driftspace of ≥ 68 cm for TOF is capable of identifying quarks at any speed. Also for any long living heavy particle the charge and the mass can be determined if the momentum p_H is sufficiently low. For particles with charge e and a mass $M_H \geq 2M_{\text{prot}}$ the rejection rate versus π , K and p is 10^{-2} at $p_H \approx 0.8 M_H$, and is better at lower momenta. Using 3 or 4 consecutive gaps improves considerably on the rejection rate.

ACKNOWLEDGEMENT

We appreciate the help and support we had from various people, in particular from W. Zimmermann in designing the smaller signal selecting circuit and from B. French, J. Engler, B. Naroska, D. Notz and H. Niebergall during the test runs at CERN.

No. of consecutive gaps	W(π ,p)(%) calculated, electronic noise		experimental
	ignored	included	
1	10	11	12
2	4	4	4
4	~ 1/2	~ 1/2	-

Table 1: Probability $W(\pi,p)$ for a pion to give an ionization like 68% of protons, at the same momentum of 1 GeV/c.

References

1. Gerhard Knies and David Neuffer; Nucl. Instr. Meth. 120 (1974) 1
2. J. Engler, B. Friend, W. Hofmann, H. Keim, R. Nickson, W. Schmidt-Parzefall, A. Segar, M. Tyrrell, D. Wegener, T. Willard, K. Winter; Nucl. Instr. Meth. 120, (1974) 157
3. W. J. Willis and V. Radeka; Nucl. Instr. Meth. 120, (1974) 221
4. G. Knies, Proceedings of the DETECTOR MEETING of DESY, October 2/3, 1975, DESY F-75/1, p.11
5. W. F. Schmidt (HMI Berlin) private communication
6. Argon N5.7, from CARBA AG, Zürich.

Figure Captions

Fig.1: Photography (a) and schematic drawing (b) of the double gap chamber.

Fig.2: Schematic of the electronics.

Fig.3: Drift time for electrons in liquid argon with methane admixtures (from Ref.5)

Fig.4: Experimental set up (not to scale).

Fig.5a: 1 GeV/c π^- ionization spectrum from the double gap. The broken line indicates the shape measured with a single gap.

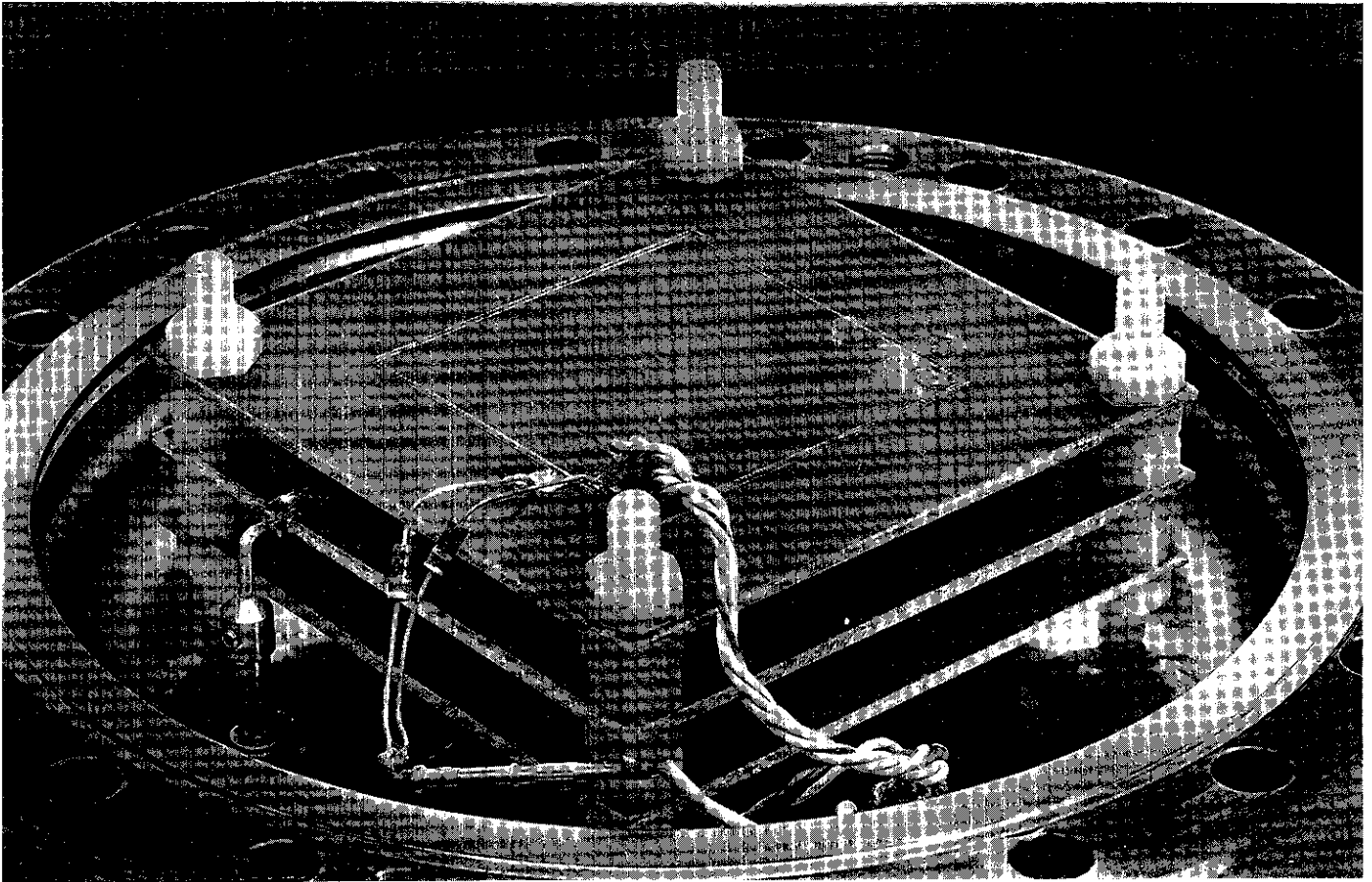
Fig.5b: 1 GeV/c π^- ionization spectrum from a single gap.

Fig.6: Ionisation spectrum of the positive beam, using the double gap chamber.

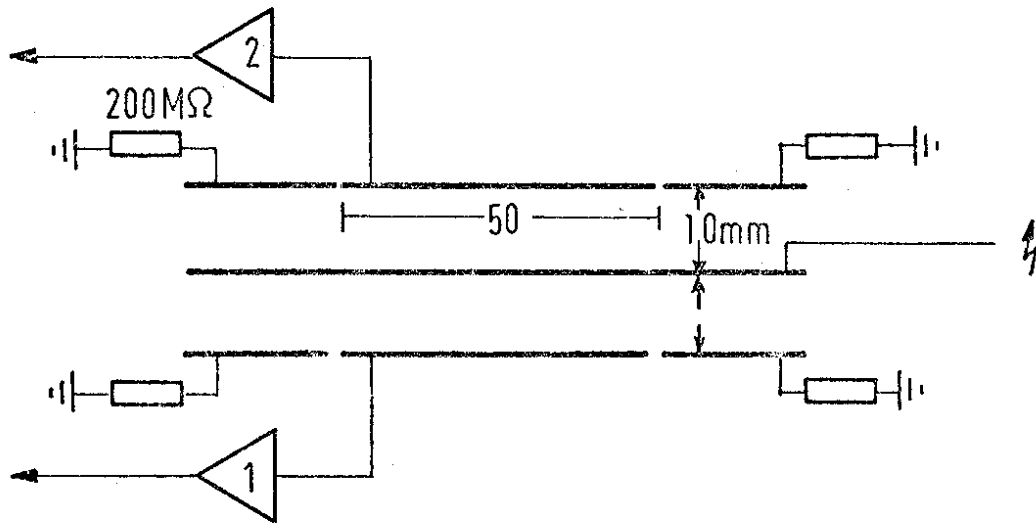
Fig.7: Ionisation spectrum of the positive beam at 1 GeV/c:
 (a) from the double gap chamber and (b) from a single gap.
 The broken line indicates the shape of the pion contribution as measured with the π^- beam.

Fig.8: Difference $\Delta(p,\pi)$ between proton and pion peak position in units of FWHM of the pion peak. The "error" bars indicate the (asymmetric) σ -width of the proton peak. The curve describes the theoretical momentum dependence of the peak difference.

Fig.9: Probability $W(\pi,p)$ for a pion to give an ionization like 68% of protons at the same momentum. The error bars reflect the uncertainty in the width of the ionization containing 68% of the protons.



a)



b)

Fig.1: Photography (a) and schematic drawing (b) of the double gap chamber.

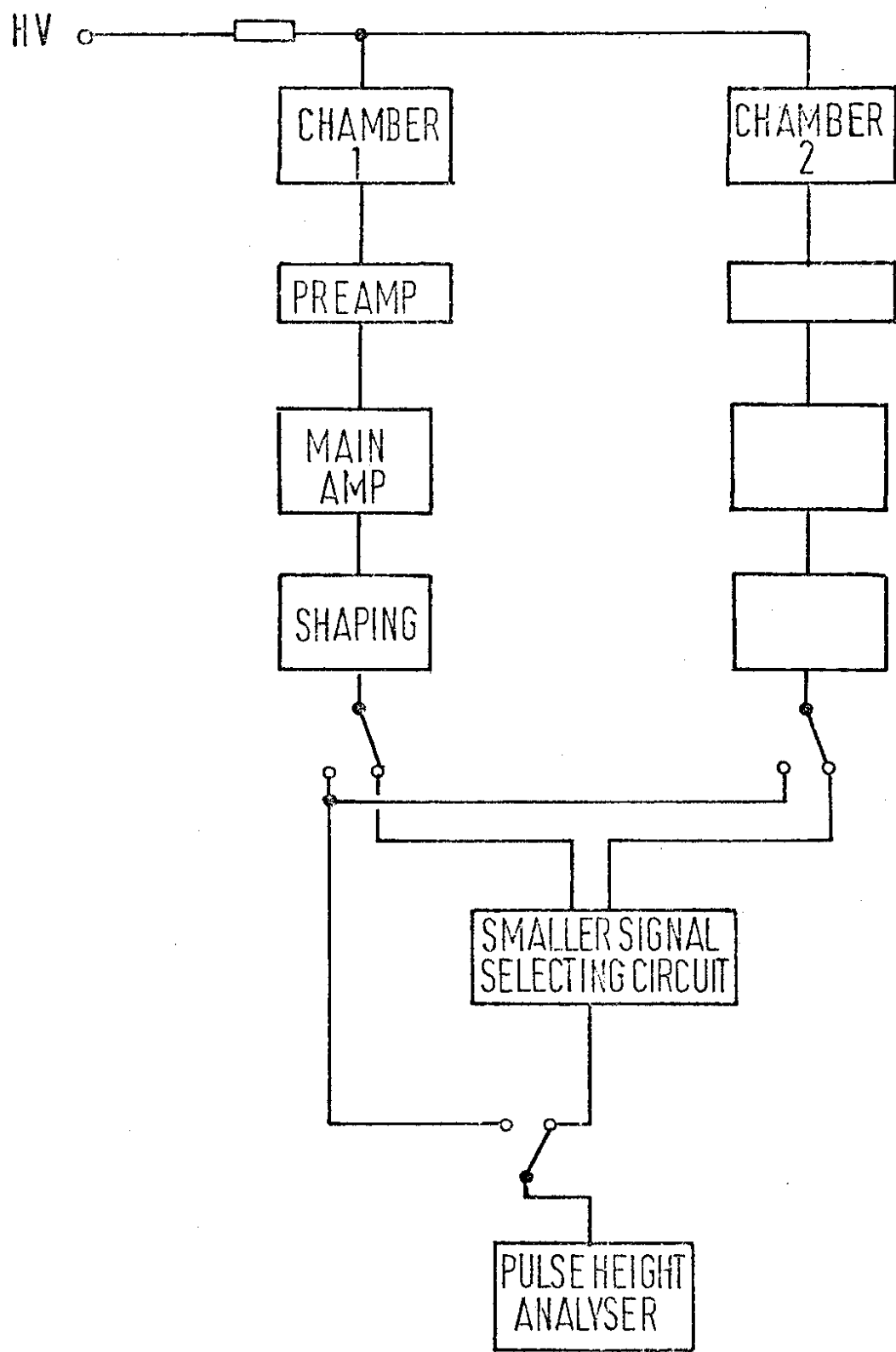


Fig.2 Schematic of the Electronics

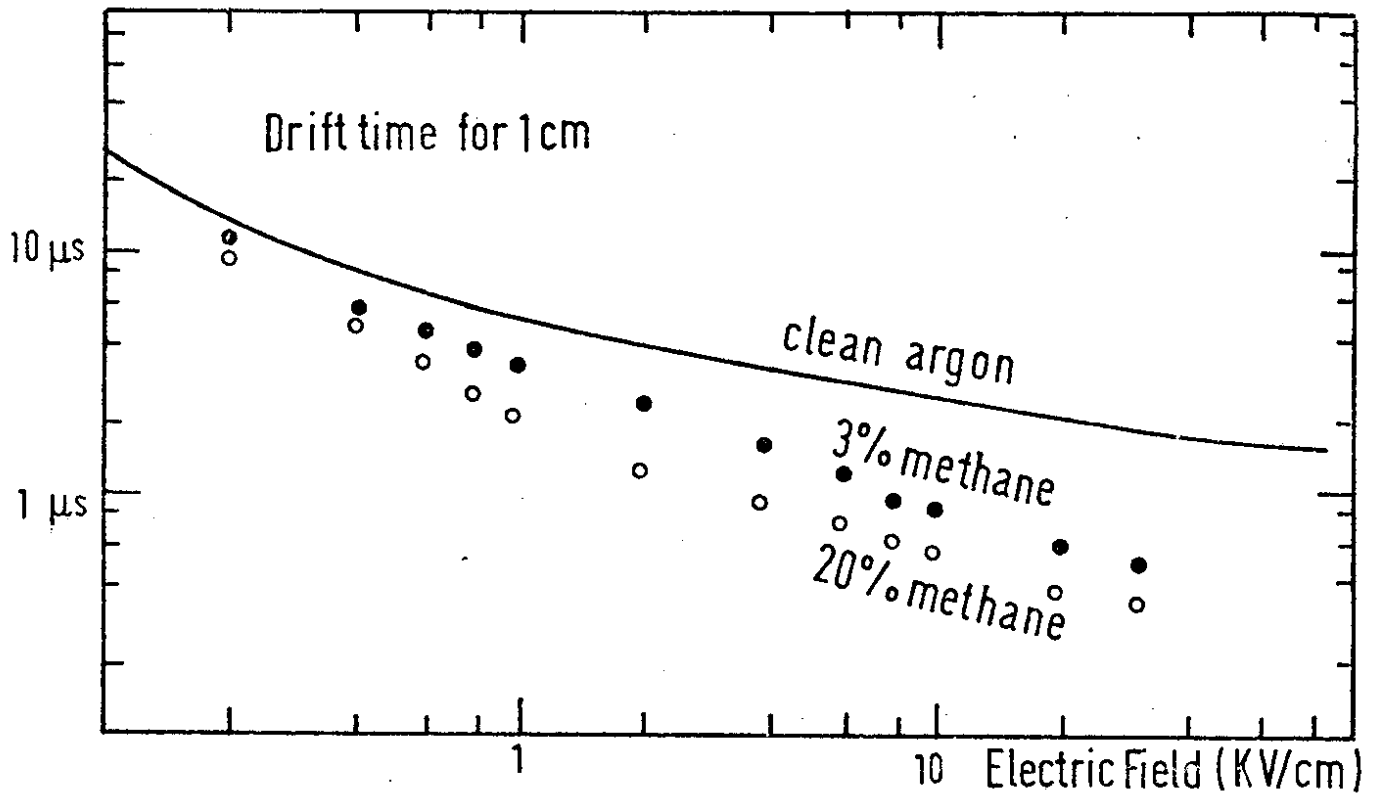


Fig.3 Drift time for electrons in liquid argon with methane admixtures (from Ref.5)

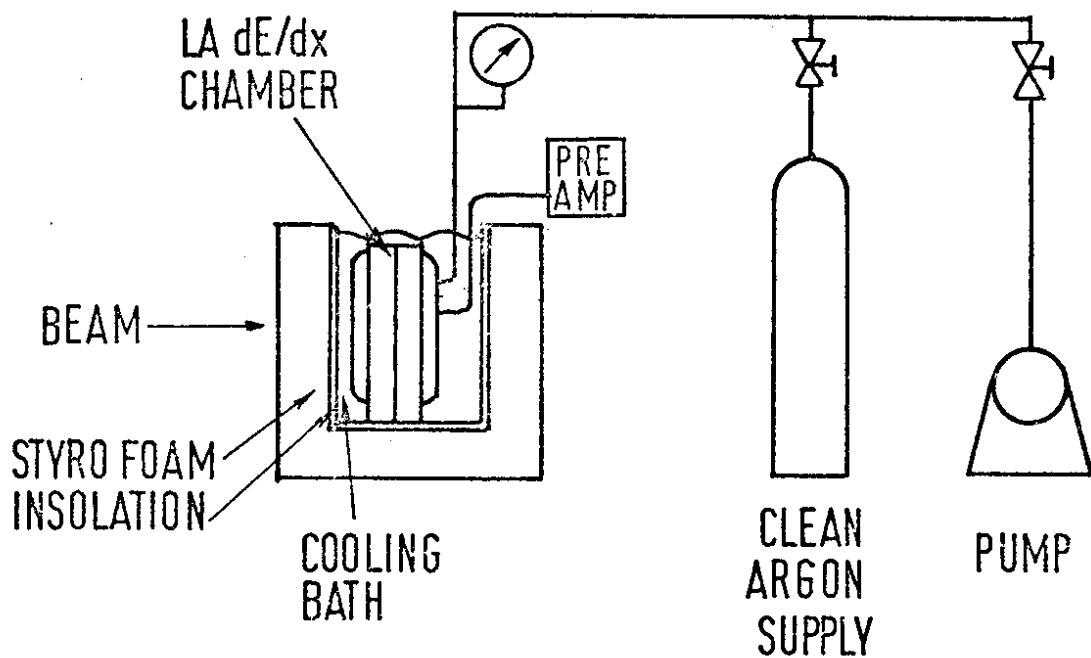


Fig.4 Experimental set up (not to scale)

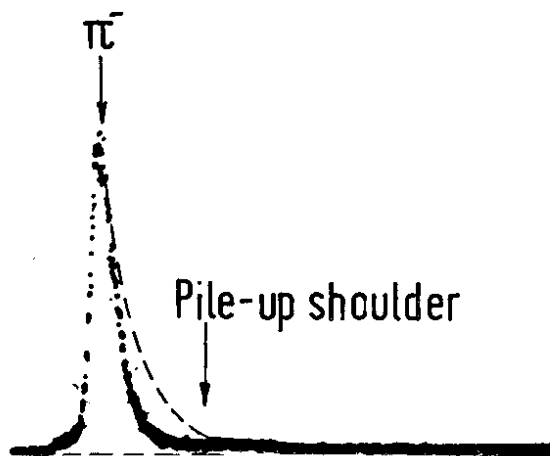


Fig.5a: 1 GeV/c π^- ionization spectrum from the double gap. The broken line indicates the shape measured with a single gap.

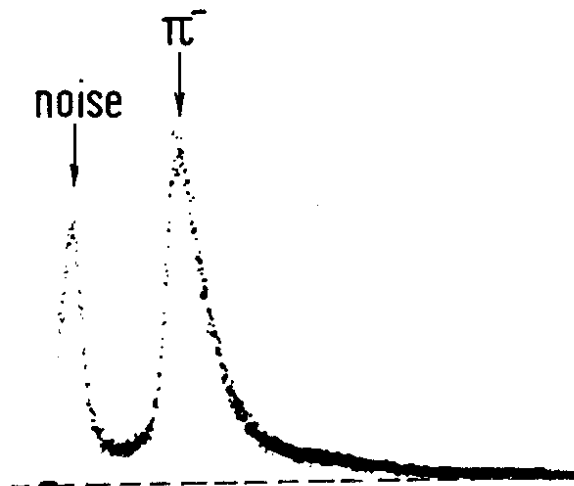


Fig.5b: 1 GeV/c π^- ionization spectrum from a single gap.

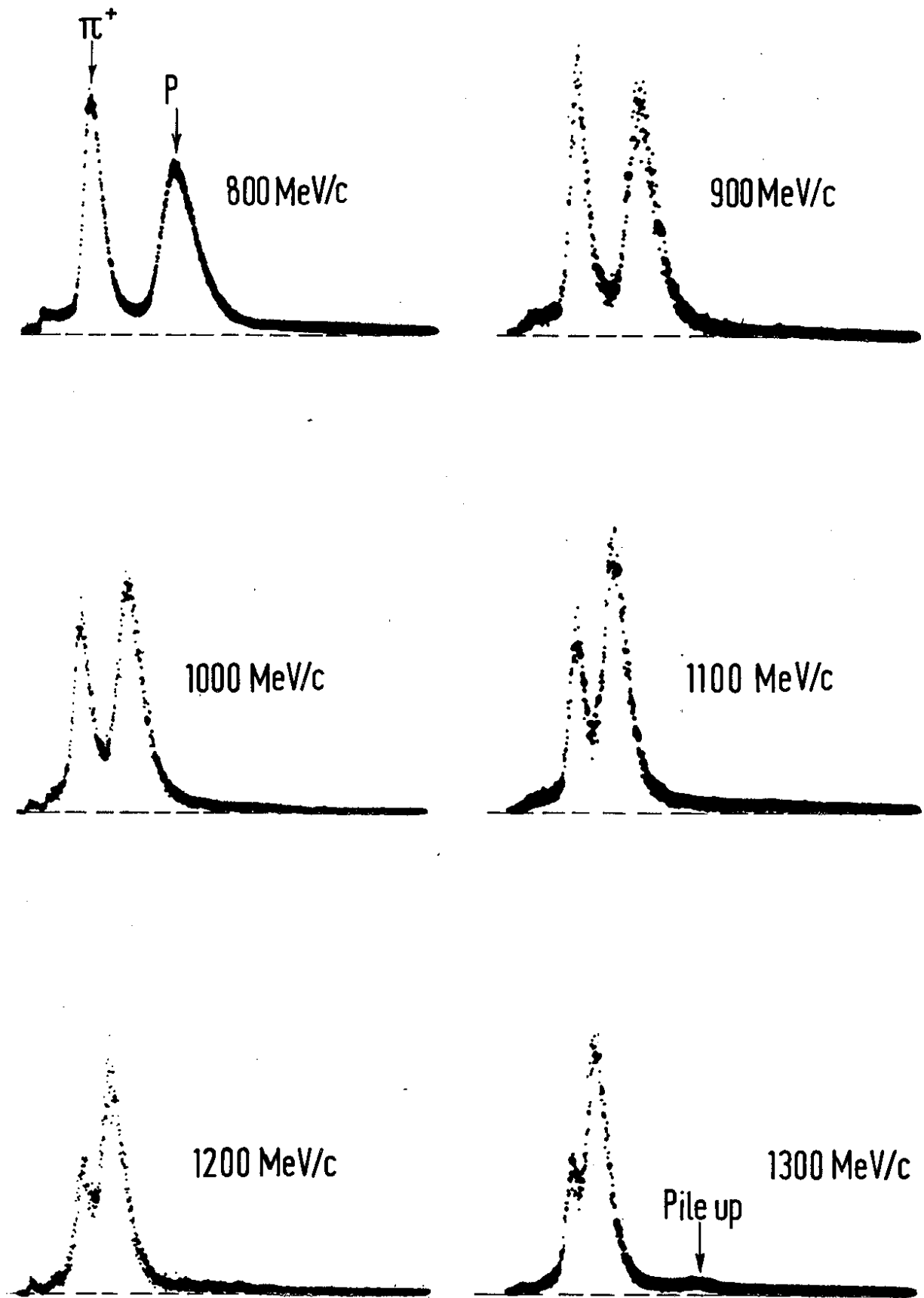


Fig.6: Ionisation spectrum of the positive beam, using the double gap chamber

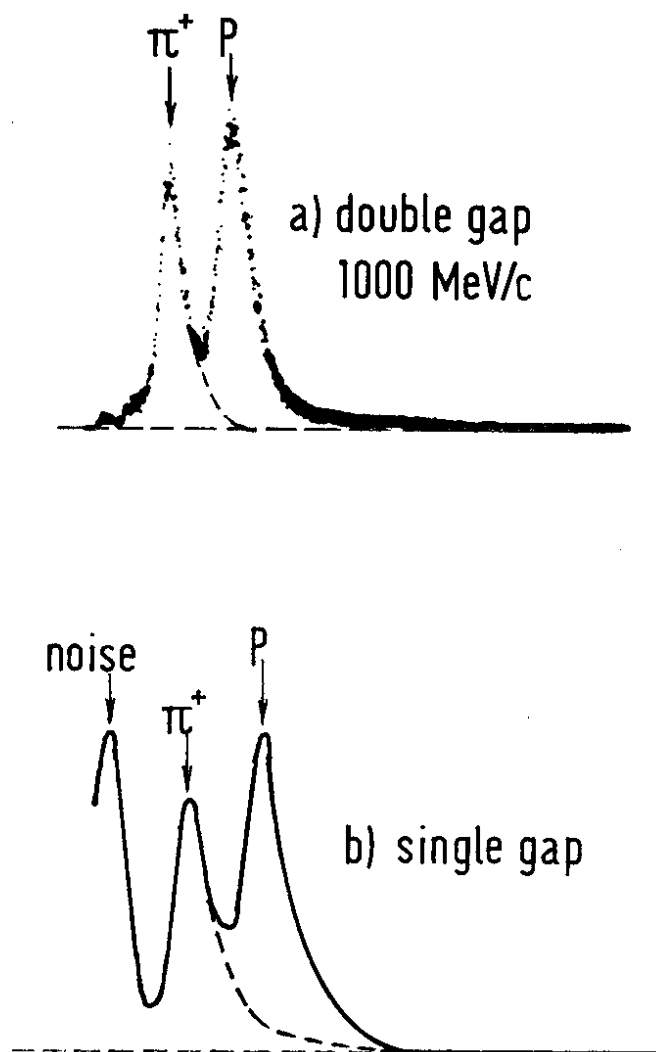


Fig.7: Ionisation spectrum of the positive beam at 1 GeV/c:
 (a) from the double gap chamber and (b) from a single gap.
 The broken line indicates the shape of the pion contribution
 as measured with the π^- beam.

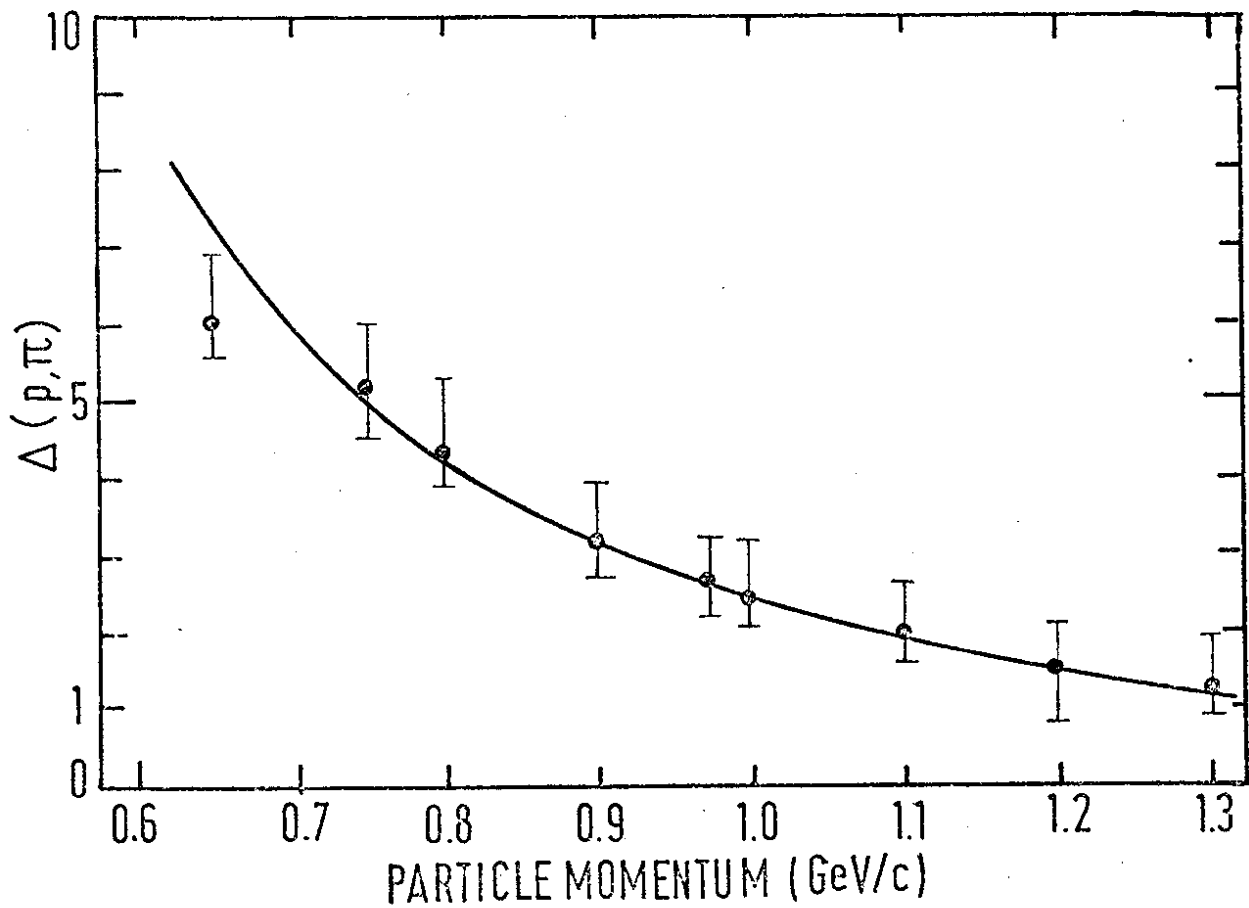


Fig. 8: Difference $\Delta(p, \pi)$ between proton and pion peak position in units of FWHM of the pion peak. The "error" bars indicate the (asymmetric) σ -width of the proton peak. The curve describes the theoretical momentum dependence of the peak difference.

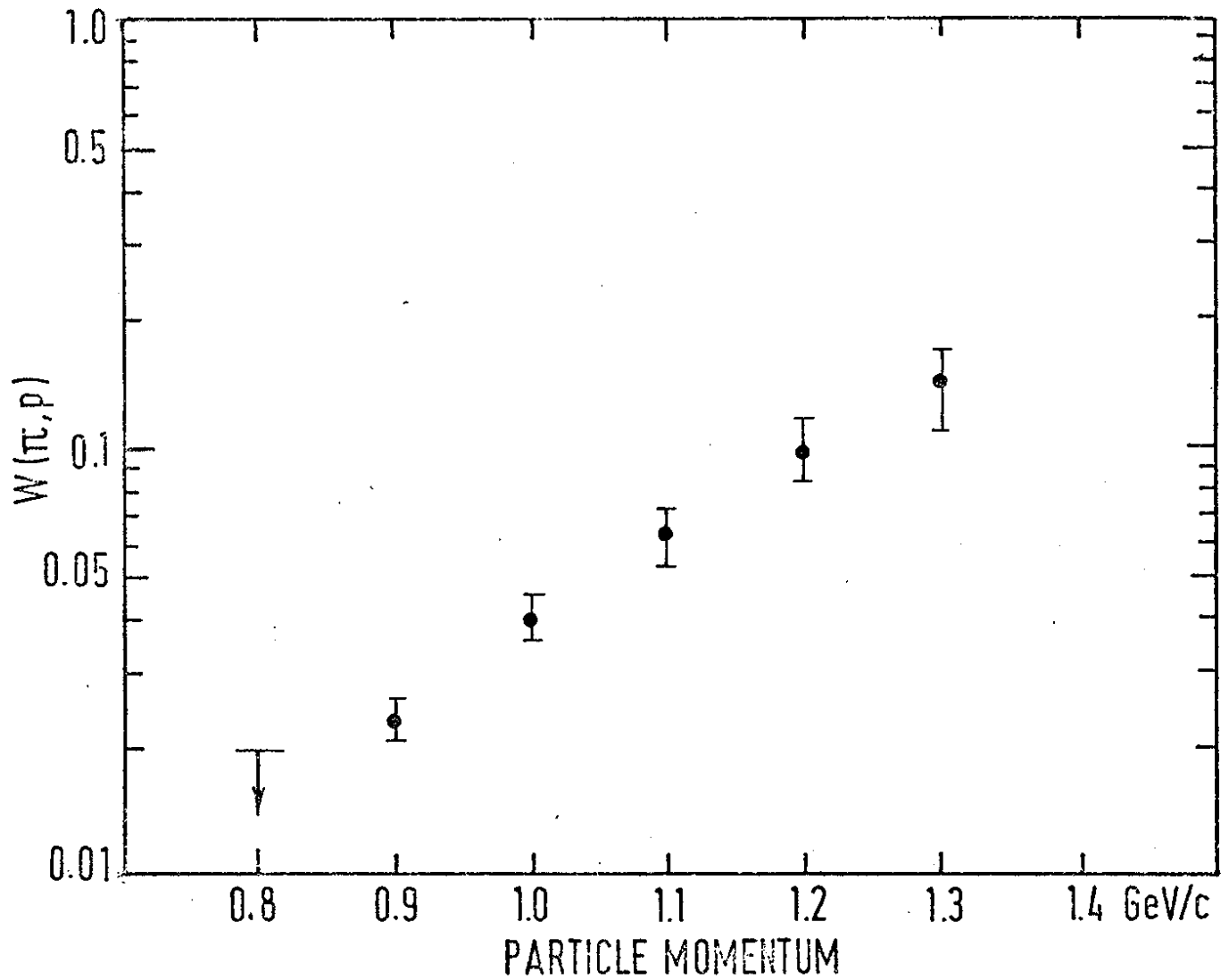


Fig.9: Probability $W(\pi, p)$ for a pion to give an ionization like 68% of protons at the same momentum. The error bars reflect the uncertainty in the width of the ionization containing 68% of the protons.